

## ***Supporting Information for the manuscript***

### **Rationally designed dual cocatalysts on ZnIn<sub>2</sub>S<sub>4</sub> nanoflower for photoredox coupling of benzyl alcohol oxidation with H<sub>2</sub> evolution**

Yu Wei<sup>a</sup>, Jun Wang<sup>a</sup>, Yong-Hui Wu<sup>a</sup>, Wei-Ya Huang<sup>a</sup>, Kai Yang<sup>a</sup>, Jia-Lin Zhang<sup>a</sup>, Kang-Qiang Lu<sup>a\*</sup> and Bin Han<sup>b\*</sup>

<sup>a</sup> Jiangxi Provincial Key Laboratory of Functional Molecular Materials Chemistry, School of Chemistry and Chemical Engineering, Jiangxi University of Science and Technology, Ganzhou, 341000, PR China

<sup>b</sup> Key Laboratory for City Cluster Environmental Safety and Green Development of the Ministry of Education, School of Ecology, Environment and Resources, Guangdong University of Technology, Guangzhou, 510006, PR China

\*To whom correspondence should be addressed

E-mail: [kqlu@jxust.edu.cn](mailto:kqlu@jxust.edu.cn); [hanbin@gdut.edu.cn](mailto:hanbin@gdut.edu.cn)

## **Synthetic procedures and characterization of products**

### **1. Synthesis of ZnIn<sub>2</sub>S<sub>4</sub> (ZIS)**

ZIS was prepared by a hydrothermal method. In a typical procedure, Zn(NO<sub>3</sub>)<sub>2</sub>·6H<sub>2</sub>O (1 mmol), InCl<sub>3</sub> (2 mmol) and CTAB (0.7 mmol) were dissolved in 30 mL of deionized (DI) water by stirring 0.5 h to form a homogeneous transparent solution. Then, excessive sulfur source TAA (8 mmol) was added into the above mixture solution. After being stirred for another 0.5 h, the mixture solution was transferred into a 50 mL Teflon-lined stainless-steel room maintained at 160 °C for 16 h. The product is cooled to room temperature in an autoclave and recovered by filtration and washed with deionized (DI) water and absolute ethanol several times, respectively. The final sample was fully dried at 60 °C in vacuum.

### **2. Synthesis of pure GO**

GO was synthesized by a modified Hummers' method. In detail, 10 g graphite powder (supplied from Qingdao Zhong tian Company, China) was put into 230 mL concentrated H<sub>2</sub>SO<sub>4</sub> under moderate stirring. Then, 30 g KMnO<sub>4</sub> was added gradually under stirring and the solution was cold below 5 °C in an ice bath. After that, the solution was heated to 35 °C in a water-bath and kept stirring for 2 h. Then, the mixture was diluted with 500 mL DI water in an ice bath to keep the temperature below 5 °C. Shortly after the further diluted with 1.5 L of DI water, 80 mL 30% H<sub>2</sub>O<sub>2</sub> was then added into the mixture. The mixture was centrifuged and washed with 1:10 HCl aqueous solution to remove metal ions followed by DI water to remove the acid. After that, the mixture was dialyzed for one week and the final GO sample was obtained after full sonication.

### **3. Synthesis of ZnIn<sub>2</sub>S<sub>4</sub>-GR (ZIS-GR)**

ZIS With the exception of adding graphene additional, ZIS-GR was prepared in the same manner as ZIS.

### **4. Synthesis of ZnIn<sub>2</sub>S<sub>4</sub>-Ni<sub>2</sub>P (ZIS-Ni<sub>2</sub>P)**

ZIS-Ni<sub>2</sub>P were prepared by an insitu photochemical deposition strategy. Typically, 60 mg of the prepared ZIS were first dispersed in a 20 mL DI by sufficient sonication, followed by addition of a calculated amount of Ni(NO<sub>3</sub>)<sub>2</sub>·6H<sub>2</sub>O and NaH<sub>2</sub>PO<sub>2</sub>. After using nitrogen (N<sub>2</sub>) bubbling for 40 min to eliminate air from the mixture, the yellow suspension was illuminated under visible light ( $\lambda > 420$  nm) for 20 min with stirring. After illumination, the precipitate was recovered by filtration and washed three times with deionised water. Finally, sample was fully dried at 60 °C in vacuum.

### **5. Characterizations**

The morphological characteristics were tested through scanning electron microscopy SEM (ZEISS Sigma 500 instrument) and transmission electron microscopy TEM (Jeol JEM-2100F instrument). The determination of crystal structures was determined by X-ray diffraction (XRD) with Cu K $\alpha$  ( $\lambda = 0.15406$  nm, Bruker D8). The surface composition of the samples was determined by X-ray photoelectron spectrometer (XPS, Thermo Fisher K-Alpha). The nitrogen adsorption-desorption isotherm of samples was analyzed using ASAP 2020 automatic analyzer.

The photoluminescence of the samples was analyzed by using FLS980 fluorescence spectrometer at the excitation wavelength  $\lambda=300$  nm. Furthermore, all the electrochemical measurements of the photocurrent, the electrochemical impedance spectra (EIS), the Mott–Schottky (MS), cyclic voltammetry (CV) and linear sweep voltammetry (LSV) curves were carried out in the three-electrode cell, in which Ag/AgCl was used as reference electrode, a Pt wire was used as a counter electrode and an indium in oxide (ITO) conductive glass was used with the samples as a working electrode in 0.1 M Na<sub>2</sub>SO<sub>4</sub> electrolyte (pH=7.56), all measurements were carried out on CH Instruments CHI-660E electrochemical workstation. The values relative to Ag/AgCl could be directly converted to the values vs NHE to facilitate comparison.

$$E_{NHE} = E_{Ag/AgCl} + 0.059 \times pH + E_{Ag/AgCl}^{\theta} \quad (1)$$

Contact angle measurements were carried out using the static drop method using a Fangrui Instrument Company JCY contact angle meter.

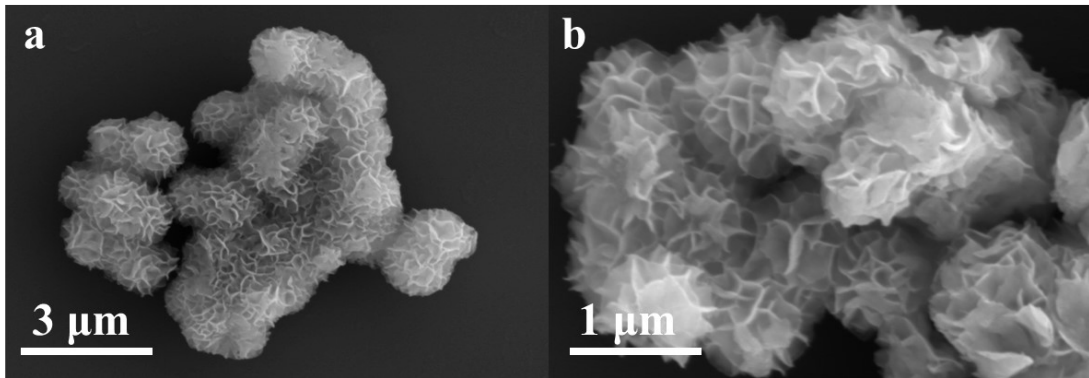


Fig. S1. FESEM images of ZIS-GR (a, b).

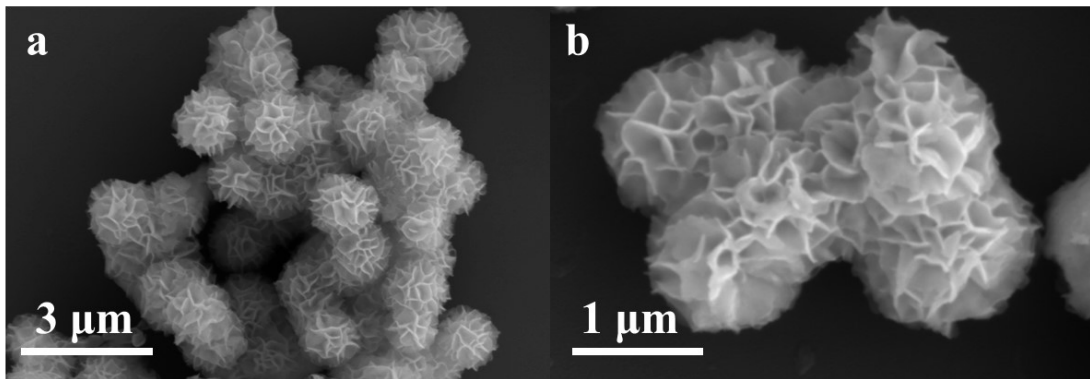


Fig. S2. FESEM images of ZIS-Ni<sub>2</sub>P(a, b).

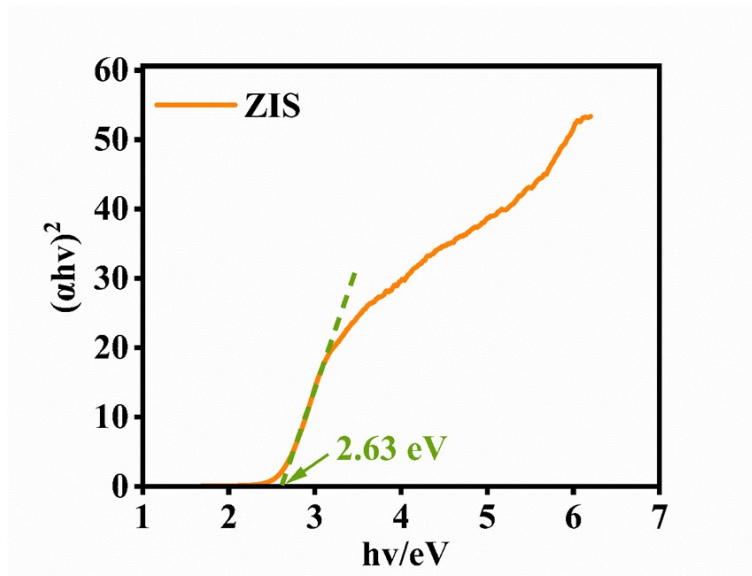
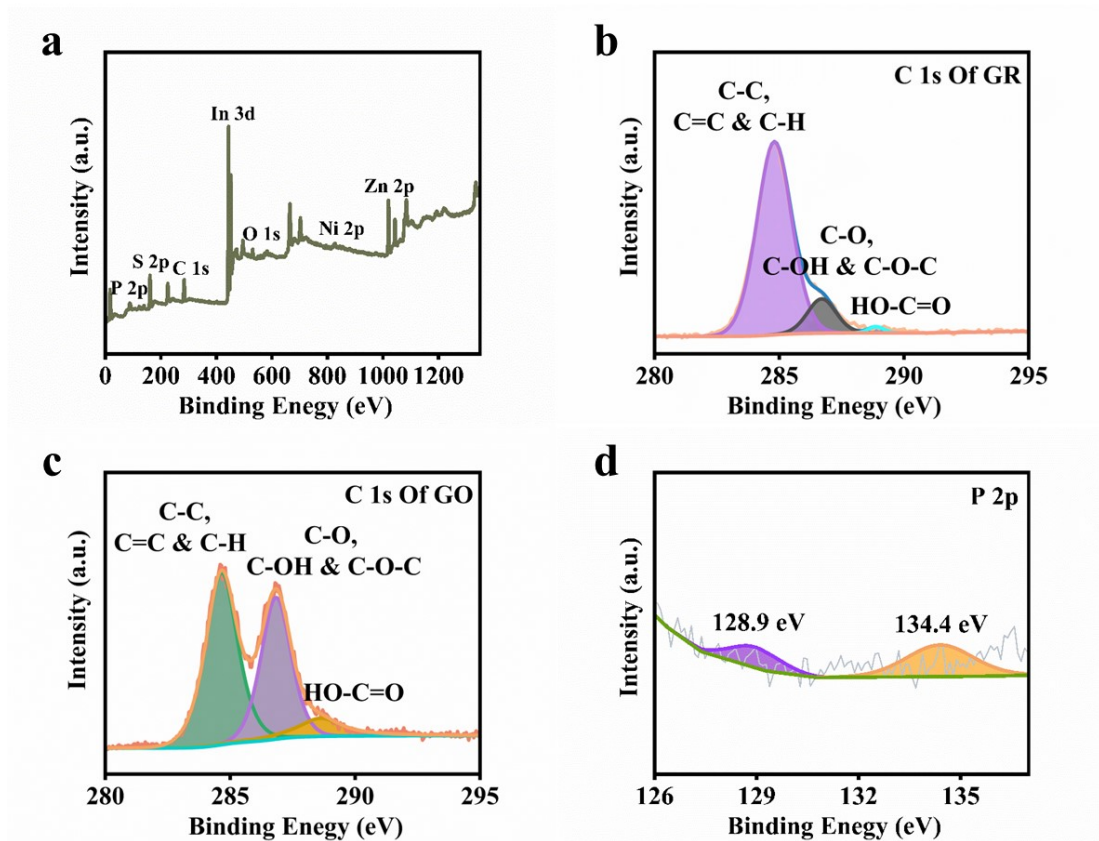
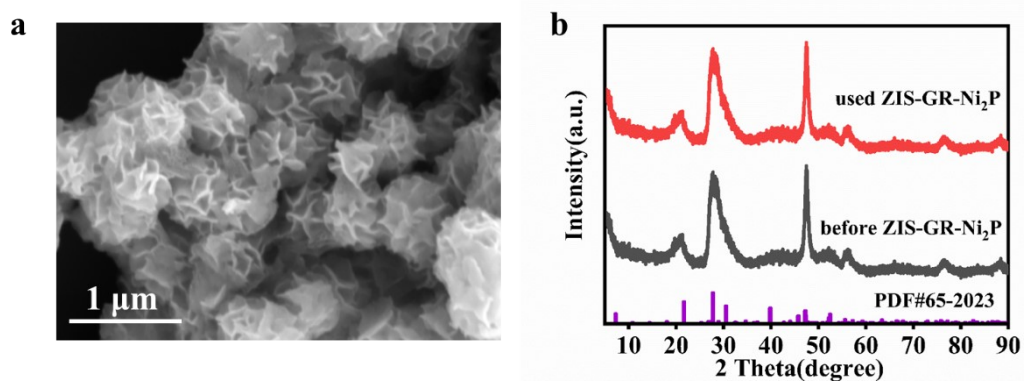


Fig. S3. Tauc plot for optical band gap of blank ZIS.



**Fig. S4.** XPS survey spectrum of ZIS-GR-Ni<sub>2</sub>P (a). XPS spectra of C 1s (c) of GR (b). XPS spectra of C 1s (c) of GO (c) and P 2p (d) of ZIS-GR-Ni<sub>2</sub>P composite.



**Fig. S5.** FESEM images of used ZIS-GR-Ni<sub>2</sub>P composites (a). X-ray diffraction (XRD) patterns of fresh and used ZIS-GR-Ni<sub>2</sub>P composites (b).

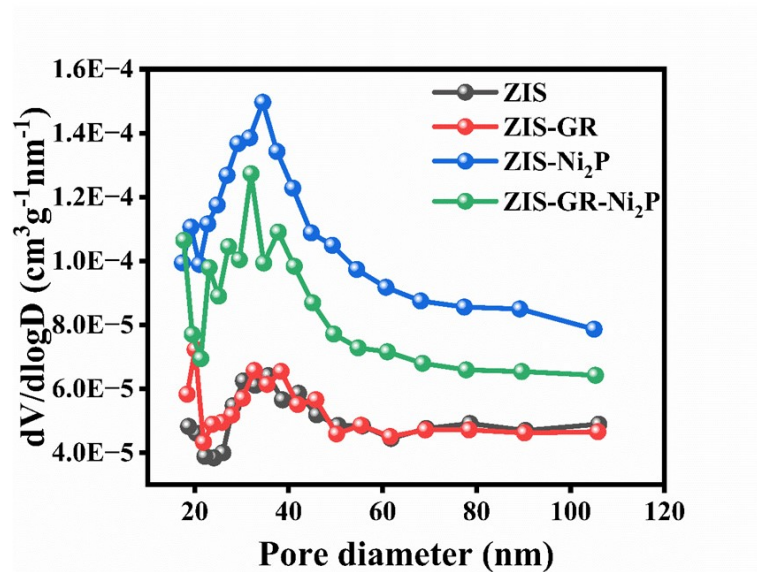


Fig. S6. Pore size distribution of ZIS, ZIS-GR, ZIS-Ni<sub>2</sub>P and ZIS-GR-Ni<sub>2</sub>P.

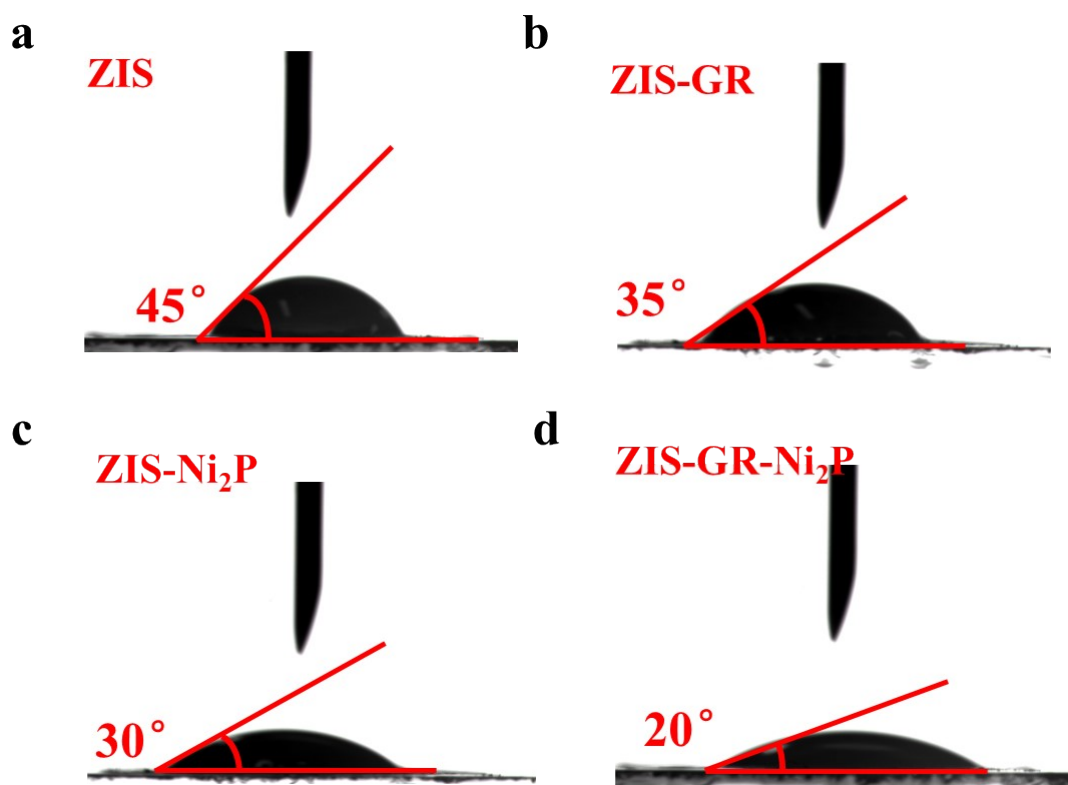


Fig. S7. Schematic diagram of the contact angles of ZIS (a), ZIS-GR (b), ZIS-Ni<sub>2</sub>P (c) and ZIS-GR-Ni<sub>2</sub>P (d) with droplets.

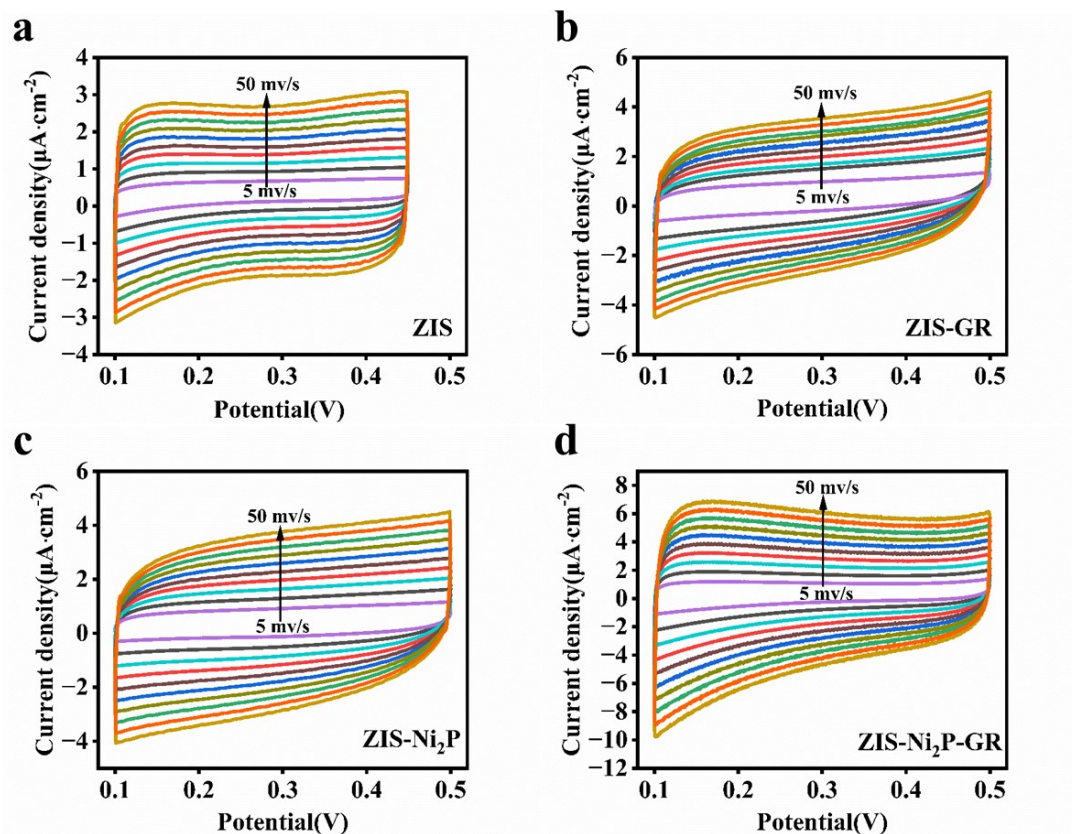


Fig. S8. CV curves of ZIS (a), ZIS-GR (b), ZIS-Ni<sub>2</sub>P (c) and ZIS-GR-Ni<sub>2</sub>P (d).

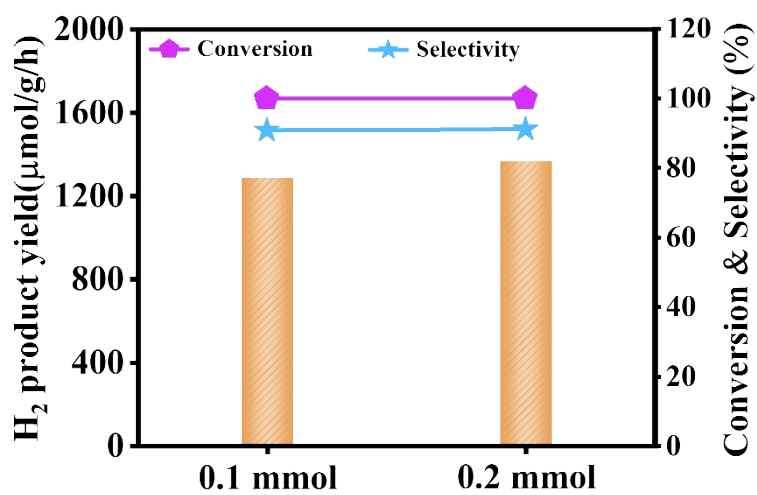
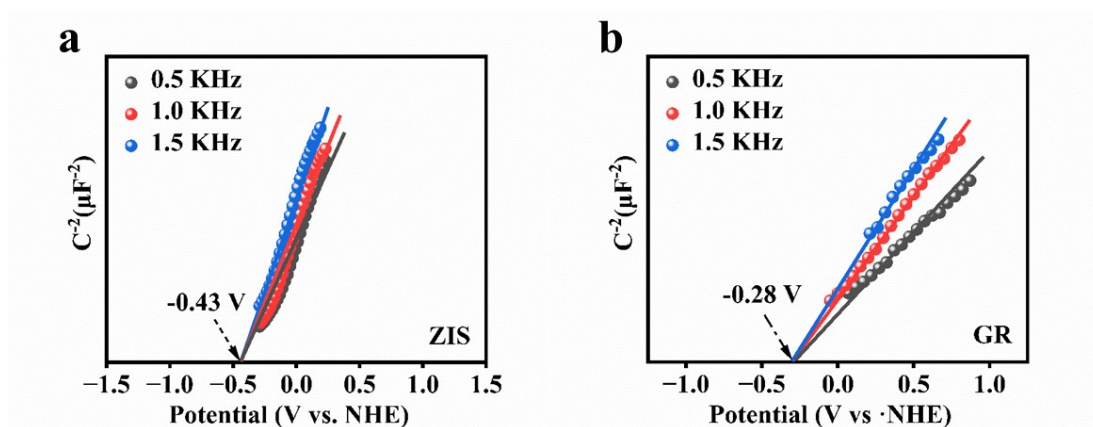


Fig. S9. Results of experiments with different BA concentration over ZIS-GR-Ni<sub>2</sub>P.



**Fig. S10.** Mott-Schottky curve of ZIS (a). Mott-Schottky curve of GR (b).



**Table S1.** Comparison the performance of benzyl alcohol oxidation to benzaldehyde and simultaneous hydrogen production

| Catalyst  | Conversion /% | Selectivity/ % | H <sub>2</sub><br>( $\mu\text{mol/g/h}$ ) | Light source                              | Reference |
|---|---------------|----------------|---|---|-----------|
| ZnIn <sub>2</sub> S <sub>4</sub> -GR-Ni <sub>2</sub> P                  | 100           | 90.9           | 1287.8                                    | 300 W Xe lamp<br>( $\lambda \geq 420$ nm) | This work |
| Ni/Zn <sub>0.5</sub> Cd <sub>0.5</sub> S                                | 40.4          | 57.7           | 284.8                                     | 300 W Xe lamp<br>( $\lambda \geq 420$ nm) | 1         |
| Ni: ZnIn <sub>2</sub> S <sub>4</sub>                                    | 97.2          | 92.8           | 36.5                                      | 300 W Xe lamp<br>( $\lambda \geq 400$ nm) | 2         |
| Pt-g-C <sub>3</sub> N <sub>4</sub>                                      | 40            | 90             | 51  | 300 W Xe lamp<br>( $\lambda \geq 400$ nm) | 3         |
| NCNCN <sub>x</sub> -GO-NiP  | 22.1          | 100            | 7.19                                      | AM 1.5 G<br>100 mW cm <sup>-2</sup>       | 4         |
| ZnS-Ni <sub>x</sub> S <sub>y</sub>                                      | 42.1          | 90.5           | 176.6                                     | 500 W Xe lamp<br>( $\lambda \geq 200$ nm) | 5         |
| ZnCo <sub>2</sub> S <sub>4</sub> /Zn <sub>0.2</sub> Cd <sub>0.8</sub> S | 54.3          | 92.2           | 45.1                                      | 300 W Xe lamp<br>( $\lambda \geq 420$ nm) | 6         |
| ZnTi-LDH  | 61            | 77             | -   | 300 W Xe lamp<br>( $\lambda \geq 400$ nm) | 7         |
| Zn <sub>3</sub> In <sub>2</sub> S <sub>6</sub> @10%ZnO                  | 91.3          | 88.6           | -   | 300 W Xe lamp<br>( $\lambda \geq 400$ nm) | 8         |

**Table S2.** Summary of the inductively coupled plasma optical emission spectroscopy (ICP-OES) analysis results of the samples of ZIS-GR-Ni<sub>2</sub>P composite after photocatalytic reaction.

| Sample                   | Zn <sup>2+</sup> (ppm) | Ni <sup>2+</sup> (ppm) |
|--------------------------|------------------------|------------------------|
| ZIS-GR-Ni <sub>2</sub> P | 1.56                   | Negligible             |

**Table S3.** BET Surface area (SBET), pore diameter (Dp) and pore volume (Vp) of pure ZIS, ZIS-GR, ZIS-Ni<sub>2</sub>P, and ZIS-GR-Ni<sub>2</sub>P samples.

| Samples                  | BET surface area(m <sup>2</sup> ·g <sup>-1</sup> ) | Pore Volume(cm <sup>3</sup> ·g <sup>-1</sup> ) | Pore Size(nm) |
|--------------------------|--|--|---------------|
| ZIS                      | 8.8303   | 0.044719                                       | 183.7451      |
| ZIS-GR                   | 9.1171   | 0.046028                                       | 201.9414      |
| ZIS-Ni <sub>2</sub> P    | 12.2451  | 0.061956                                       | 202.3882      |
| ZIS-Ni <sub>2</sub> P-GR | 13.7705  | 0.063256                                       | 202.5736      |

## References

- 1 L. Zhang, D. Jiang, R. M. Irfan, S. Tang, X. Chen and P. Du, *J. Energy Chem.*, 2019, **30**, 71–77.
- 2 Q. Lin, Y.-H. Li, M.-Y. Qi, J.-Y. Li, Z.-R. Tang, M. Anpo, Y. M. A. Yamada and Y.-J. Xu, *Appl. Catal. B Environ.*, 2020, **271**, 118946.
- 3 F. Li, Y. Wang, J. Du, Y. Zhu, C. Xu and L. Sun, *Appl. Catal. B Environ.*, 2018, **225**, 258–263.
- 4 H. Kasap, R. Godin, C. Jeay-Bizot, D. S. Achilleos, X. Fang, J. R. Durrant and E. Reisner, *ACS Catal.*, 2018, **8**, 6914–6926.
- 5 H. Hao, L. Zhang, W. Wang, S. Qiao and X. Liu, *ACS Sustain. Chem. Eng.*, 2019, **7**, 10501–10508.
- 6 C. Li, S. Shan, K. Ren, W. Dou, C. He and P. Fang, *Int. J. Hydrog. Energy*, 2022, **47**, 38951–38963.
- 7 J. Zou, Z. Wang, W. Guo, B. Guo, Y. Yu and L. Wu, *Appl. Catal. B Environ.*, 2020, **260**, 118185.
- 8 J. Zhang, S. Meng, X. Ye, C. Ling, S. Zhang, X. Fu and S. Chen, *Appl. Catal. B Environ.*, 2017, **218**, 420–429.